Densification and Microstructural Evolution of TiO_2 Films Prepared by Sol−Gel Processing

Matthias Bockmeyer[†] and Peer Löbmann*[,‡]

Lehrstuhl für die Chemische Technologie der Materialsynthese, Röntgenring 11, D-97070 Würzburg, Germany, and Fraunhofer-Institut für Silicatforschung, Neunerplatz 2, D-97082 Würzburg, Germany

Received September 12, 2005. Revised Manuscript Received May 10, 2006

Soluble precursor powders for TiO_2-coating solutions were prepared and dissolved in solvent mixtures containing ethanol and 1,5-pentanediol in different ratios. Materials isolated by rotational evaporation of the sols (sol powders) and scraping of films deposited by dip-coating (film powders) were annealed at different temperatures and thoroughly characterized in order to investigate the influence of solvent composition and drying conditions on the film densification. Organic groups present in the precursor are partially exchanged during solvent evaporation. The chemical composition of these materials has a significant influence on the respective densification behavior and properties such as surface area and porosity. This observation can be correlated to the evolution of the crystalline polymorphs of TiO_2, anatase, and rutile. The large area-to-volume ratio and the presence of air moisture during film drying cause significant chemical and microstructural differences between film powders and sol powders prepared by rotational evaporation. The rapid solvent evaporation in films leads to a fast densification and the inclusion of organic groups, which cause the transient presence of CO_2 entrapped in closed pores upon sintering. The conclusions drawn from the characterization of the different powders are the basis to understanding and avoiding the formation of defects on a microscopic level.

1. Introduction

Sol−gel processing[1] has become a versatile method for preparing thin films on an industrial scale. Especially for the coating of polymers, a vast variety of hybrid organic−inorganic compositions have been developed[2,3] that provide, for example, scratch resistance, coloration, specific barrier properties, electrical conductivity, and modified surface energy.

Purely inorganic sol−gel films mostly require curing temperatures exceeding 400 °C and thus have to be applied to substrates such as glass, metals,[4] or ceramics[5], which are thermally more stable than organic polymers. Highly uniform films for optical applications (filters, antireflective coatings) can be prepared on large areas using cost-efficient production facilities by, for example, dip-coating.[6−8]

On the microscopic level, however, material deposition results from a complex interwoven sequence of interacting processes. The liquid film is obtained by transfer of the coating solution to a moving substrate, which is governed by numerous factors such as withdrawal rate, sol viscosity, and density.[9] The more-volatile components of the sol will evaporate first, increasing the concentration of water and catalyst, which in turn will promote further hydrolysis and condensation reactions of precursor particles and molecules.[10] Subsequently, gelling will occur, transforming the viscous liquid film to a viscoelastic gel that is tightly attached to the moving substrate. Residual solvent will escape from the pores; additionally, air moisture may be absorbed by the still-reactive gel. Drying and continued condensation reactions within the network result in further shrinkage, which is unhindered only perpendicularly to the substrate. Tensile stresses will build up in the plane of the surface.[9] If these forces exceed the cohesion of the film, it will crack, during either drying or final thermal curing.[11,12]

Even though a considerable level of understanding of the respective processes has been established and general strategies for avoiding stress-related damage have been developed,[9,13−15] there are fewer reports on the relationship among the microstructure of films and their densification

* Corresponding author. Phone: 49 (0)931 4100-404. Fax: 49 (0)931 4100-559. E-mail: loebmann@isc.fhg.de.
[†] Lehrstuhl für die Chemische Technologie der Materialsynthese.
[‡] Fraunhofer-Institut für Silicatforschung.

(1) Brinker, C.; Scherer, G. *Sol−Gel Science: The Physics and Chemistry of Sol−Gel Processing*; Academic Press: Boston, 1990.
(2) Schottner, G. *Chem. Mater.* **2001,** *13,* 3422.
(3) Schmidt, H. *Macromol. Symp.* **2000,** *159,* 43.
(4) Löbmann, P.; Jahn, R.; Seifert. S.; Sporn, D. *J. Sol−Gel Sci. Technol.* **2000**, *19,* 473.
(5) Krüger, R.; Bockmeyer, M.; Löbmann, P. *J. Am. Ceram. Soc.* **2006**, accepted.
(6) Löbmann, P.; Röhlen, P.; *J. Glass Sci. Technol.* **2003**, *76,* 1.
(7) Gombert, A.; Glaubitt, W.; Rose, K.; Dreibholz, J.; Zanke, C.; Bläsi, B.; Heinzel, A.; Horbelt, W.; Sporn, D.; Döll, W.; Wittwer, V.; Luther J. *Sol. Energy* **1998**, *62,* 177.
(8) Gombert, A.; Glaubitt, W.; Rose, K.; Dreibholz, J.; Bläsi, B.; Heinzel, A.; Sporn, D.; Döll, W.; Wittwer, V. *Thin Solid Films* **1999**, *351,* 73.
(9) Scherer, G. *J. Sol−Gel Sci. Technol.* **1997**, *8,* 353.
(10) Brinker, C.; Hurd, A.; Frye, G.; Ashley, C. *J. Non-Cryst. Solids* **1992**, *147−148,* 424.
(11) Scherer, G. *J. Non-Cryst. Solids* **1988**, *100*, 77.
(12) Caincross, A.; Chen, K.; Schunk, K.; Brinker, C.; Hurd, A. *Ceram. Trans.* **1997**, *69*, 153.
(13) Burgos, M.; Langlet, M. *J. Sol−Gel Sci. Technol.* **1999**, *16*, 267.
(14) Kozuka, H.; Takenaka, S.; Tokita, H.; Hirano, T.; Higashi, Y.; Hamatani, T. *J. Sol−Gel Sci. Technol.* **2003**, *26*, 681.
(15) Seco, A.; Goncalves, M.; Almeida, R. *Mater. Sci. Eng., B* **2000**, *76*, 193.

10.1021/cm052048n CCC: $33.50
Published on Web 08/15/2006

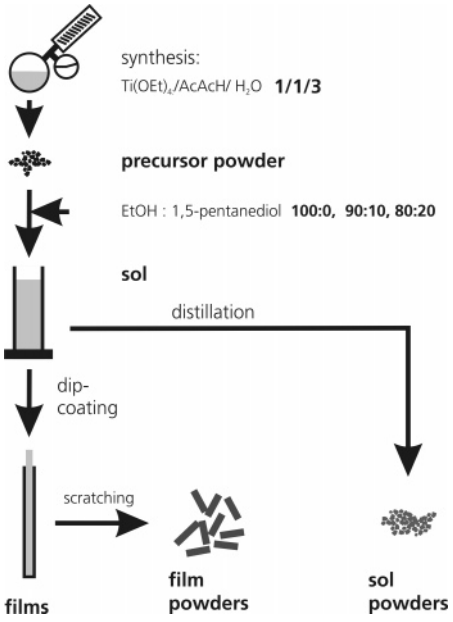

Figure 1. Illustration of different TiO_2 materials used for the characterization of the film formation and densification. See text for details.

and cracking.[16,17] This may be partially due to the limited accessibility of sufficient amounts of film material for solid-state characterization.[18]

The use of novel soluble precursor powders has proven to be beneficial for the production of TiO_2 thin films on an industrial level.[6] When titanium alkoxides are chelated with acetylacetone and hydrolyzed, all volatile components may be distilled off under certain conditions, resulting in amorphous, soluble precursor powder that is infinitely stable under ambient conditions. It is possible to employ different solvents or solvent mixtures for preparing TiO_2 coating solutions; their stability and the resulting film quality depends both on the respective powder and the solvent composition.[19]

In addition to the practical advantages there are some new analytical perspectives. The precursor powders can be characterized as a function of annealing temperature. Additionally, coating solutions may be stripped off again in order to investigate the role of different solvents during a drying process (sol powders) (Figure 1). When as-dried films are scratched off a substrate, the solid-state analysis of these film powders provides valuable information on the effect of air moisture and the unidirectional densification during drying. The microstructure of annealed film powders is finally the best match to the microstructure of sintered films, which unfortunately cannot be isolated because of their strong adhesion to the substrates. It is possible to isolate sufficient amounts of these materials to, for example, perform N_2 sorption experiments or measure their skeletal density, which can hardly be done using thin films.

Here, we report about the influence of solvent composition on the properties of TiO_2 thin films. Results indicate that ligands of the initial precursor material are exchanged with solvent molecules during solvent evaporation. The high surface-to-volume ratio and access of air moisture during film drying determine the chemical composition of the as-prepared film, which controls shrinkage, crystallization, and defect structure of the coatings during sintering.

2. Experimental Procedure

2.1. Preparation of TiO_2 Precursor Powders and Dip-Coating Solutions. TiO_2 precursor powders were prepared from titanium tetraethoxide using acetylacetone as the chelating agent and water for the hydrolysis reaction in a 1:1:3 molar ratio. More-detailed information about the precursor powder synthesis and the preparation of the coating solutions was previously reported.[6,19]

2.2. Preparation of Sol Powder and Film Powder. Sol powders were obtained after rotational evaporation of all volatile components from the sols at reduced pressure (<20 mbar), with a maximum bath temperature of 80 °C. Coating powders were prepared by multiple dip-coating (~30 times, withdrawal rate of 50 cm/min) of 30 × 30 cm^2 glass plates. The drying time of each single thin sol−gel film was 10 min, and the relative humidity was kept at 30 ± 5% at 20 °C (5.2 ± 0.9 g H_2O/m^3). The multilayer gel film was then dried at 60 °C for 15 min and scraped off with a razor blade. Chemical analysis revealed that the material isolated contained neither parts of the substrate nor traces of the metallic blade. The obtained sol powders and film powders were placed in a furnace (model M110, Heraeus Instruments, Hanau, Germany) preheated to the designated temperature and held there for 60 min.

2.3. Powder Characterization. Differential thermal analysis (DTA) and thermogravimetric analysis (TGA; Setaram TAG24, Caluire, France) of the sol powder and coating powder were performed with a heating rate of 10 K/min in a dry air atmosphere. Helium pycnometry (model Accupyc 1330, Micromeritics Instrument Corp., Norcross, MA) was applied to determine the skeletal densities. Nitrogen sorption was measured with an automated volumetric analyzer (model Autosorb 3B, Quantachrome Instruments, Boynton Beach, FL). Prior to nitrogen adsorption analysis, samples were dried at 110 °C for 16 h at reduced pressure. The multipoint method was used to determine the specific surface area according to Brunauer, Emmet, and Teller (BET). Powder X-ray diffractometry (XRD; model Stadi P Stoe, Darmstadt, Germany) was used to verify phase development. ZnO was added as an internal standard (20 mass %), and the powders were mixed thoroughly by grinding in a mortar. FT-IR measurements of powder samples, prepared as KBr pellets, were carried out using a Magna-IR 760 spectrometer (FT-IR; Nicolet Instrument Corporation, Waltham, MA).

2.4. Thin Film Preparation. Thin films were prepared by dip-coating on borosilicate glass (Borofloat), as described elsewhere.[6,19] Preparation and drying of the films was carried out under constant humidity conditions (4.4 g H_2O/m^3, 20% RH at 24 °C) using a climate control unit.

2.5. Film Characterization. Film thickness of the thin films was calculated from UV−vis reflection spectra (UV−vis spectrometer, Shimadzu UV-3100, Kyoto, Japan) using the Swanepoel method.[20] Coatings were photographed with a light microscope (Leica DC 300, Wetzlar, Germany) using 20-fold magnification and the Leica Image Manager.

(16) Pell, W.; Delak, K.; zur Loye, H. *Chem. Mater.* **1998**, *10*, 1764.
(17) Brenier, R.; Ortéga, L. *J. Sol−Gel Sci. Technol.* **2004**, *29*, 137.
(18) Mehner, A.; Datchary, W.; Bleil, N.; Zoch, H.; Klopfstein, M.; Lucca, D. *J. Sol−Gel Sci. Technol.* **2005**, *36*, 25.
(19) Löbmann, P. *J. Sol−Gel Sci. Technol.* **2005**, *33*, 275.
(20) Diaz-Parralejo, A.; Caruso, R.; Ortiz, A.; Guiberteau, F. *Thin Solid Films* **2004**, *458*, 92.

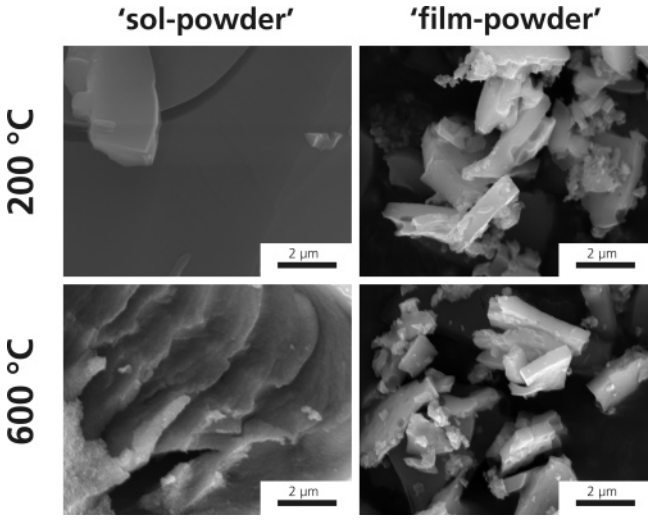

Figure 2. SEM images of sol powder (left) and corresponding film powder (right) at calcination temperatures of 200 (top) and 600 °C (bottom). Pure ethanol was used as solvent.

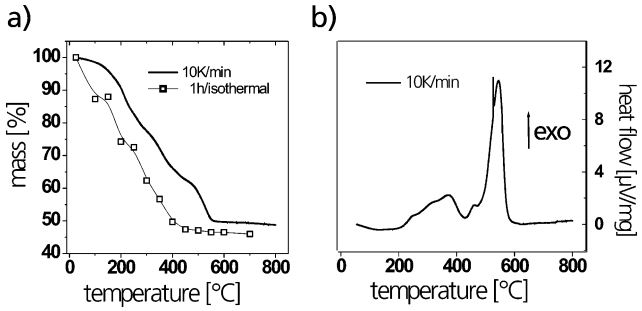

Figure 3. Thermogravimetric analysis (a) and differential thermal analysis (b) of soluble TiO_2 precursor powere synthesized using $Ti(OEt)_4$, acetylacetone, and water in a 1:1:3 molar ratio. Both experiments were performed under a dry air atmosphere with a heating rate of 10 K/min. In (a), mass losses are given (open symbols) for samples isothermally annealed for 1 h at the respective termperature. The line is drawn as a guide for the eyes.

3. Results and Discussion

In Figure 2, typical SEM images of sol-powders and film powders annealed at 200 and 600 °C are shown. Even though a qualitative difference between the coarser material prepared by simple solvent evaporation and films scraped off the substrate can be estimated, microscopic methods are obviously not suitable for qualitatively characterizing changes induced by thermal treatment. Therefore, the combination of thermal analysis, N_2 sorption, IR spectroscopy, He pyknometry, and X-ray diffraction will be used for further investigations.

3.1. Changes Induced by the Solvent: Comparison between the Precursor and Different Sol Powders. The results of representative thermogravimetric analysis (TGA) and differential thermal analysis (DTA) experiments of a soluble TiO_2 precursor powder are given in Figure 3. In our previous work,[19] the first mass loss and associated exothermal signal could be assigned to the decomposition of acetylacetonate moieties, whereas the second set of signals is due to the removal of alkoxy groups. Samples that were isothermally annealed at temperatures below 600 °C for 1 h in a preheated furnace (Figure 3a) generally achieve the same mass loss at lower temperatures than those in the experiments with constant heating rates. Even though this observation is

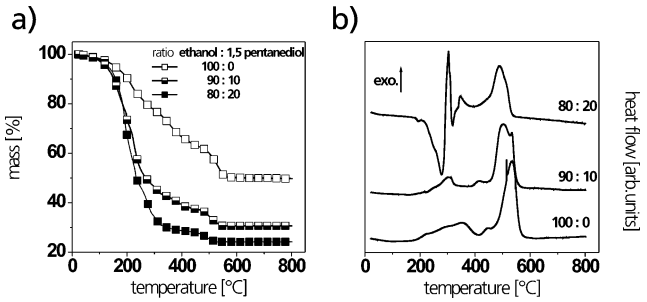

Figure 4. Thermogravimetric analysis (a) and differential themal analysis (b) of sol powders obtained from ethanolic coating solutions conating 0 (□), 10 (◒), and 20% (■) 1.5-pentanediol (compositions were 100:0, 90: 10, and 80:20, respectively). The experiments were performed under a dry iar atmosphere with a heating rate of 10 K/min.

predictable, this systematic offset must be considered when results from different experimental setups are compared.

When pure ethanol is used as solvent and all volatile components are again removed by rotational evaporation, the resulting sol powder exhibits a thermal decomposition pattern identical to that of the soluble precursor powder employed. Obviously, the initial synthesis conditions have established a stable configuration of the precursor that remains unaffected in the presence of ethanol as solvent.

This situation changes when the solvent mixture contains 1,5-pentanediol (Figure 4). In this case, the material isolated after rotational evaporation is a highly viscous liquid rather than a powder. Apparently, the vacuum conditions employed are not sufficient to completely remove the diol (bp 242 °C), as additionally indicated by higher total mass losses during thermogravimetric analysis (Figure 4a). This assumption is corroborated by the DTA measurements performed on the different residues (Figure 4b). As already mentioned, the DTA pattern of powders from purely ethanol-based sols does not differ from those of the respective precursor powder (Figure 4b). When 10% 1,5-pentanediol was present in the sol, the signals assigned to the decomposition of acetylacetonate and ethanolate groups are broadened, indicating partial replacement by the diol. When its content is increased to 20%, the first exothermal signal is superimposed by the endothermal evaporation of the diol (∼242 °C). On the basis of these observations, one could expect that 1,5-pentanediol should become enriched during drying of films and thus may maintain some plasticity of the deposited material.[14]

Measurements of the skeletal backbone densities of the powders as a function of isothermal annealing temperatures (Figure 5) provide additional insight into the influence of the solvent mixture. Sol powders prepared from purely ethanolic solutions exhibit the highest initial skeletal density, and increasing amounts of 1,5-pentanediol in the sol decrease the density of the respective material.

Upon annealing, the powders prepared from sols containing 1,5-pentanediol undergo a steeper skeletal densification than the samples from purely ethanolic sols. However, for all materials, a value of approximately 3.6 g/cm^3 is measured after treatment at 400 °C.

Above this temperature, the presence of organic residues cannot account for any differences in the backbone densities, because no significant mass loss takes place during isothermal sintering above 400 °C (Figure 3a). Nevertheless,

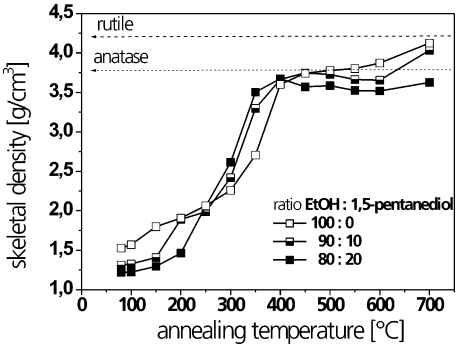

Figure 5. Skeletal differences of sol powders prepared from different sols as a function of annealing temperature. The theoretical densities of rutile (4.23 g/cm^3) and anatase (3.83 g/cm^3) are given as references.

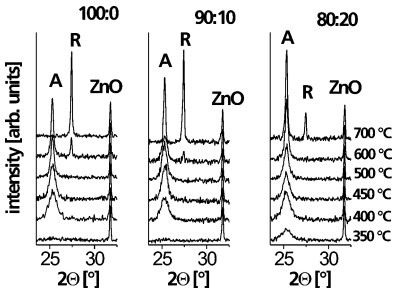

Figure 6. X-ray diffraction pattern of sol powders prepared from sols containing, from left to right, 0, 10, and 20% 1,5-pentanediol. The samples weer annealed at temperatures between 350 and 700 °C, as indicated at the right side of the figure. ZnO was used as an external standard to normalize the signal intensities; peaks assigned to anatase (A) and rutile (R) are marked individually.

powders that are treated up to 400 °C are colorless but show a grayish-to-black appearance in an intermediate temperature range and become colorless again at 700 °C. This visual observation indicates the transitional presence of small volume fractions of elementary carbon due to an incomplete oxidative decomposition of organic moieties. These small amounts obviously do not significantly contribute to the TGA results above 400 °C (Figure 3a, open symbols). Nevertheless, the increase in skeletal density correlates with the initial solvent composition; the lower the content of 1,5-pentanediol, the better the densification with increasing temperature. In turn, powders from sols with 20% diol do not reach the skeletal density expected for crystalline anatase (3.84 g/cm^3), even after sintering at 700 °C.

Further investigations by X-ray diffraction experiments were carried out that reveal different contents of crystalline phases (Figure 6) above 500 °C. Even though only anatase is found as a product of the initial phase of crystallization for all samples, rutile starts to crystallize at 600 °C and becomes the dominating phase at 700 °C for samples that contained no or only 10% pentanediol. In contrast to this, if the initial sol comprised 20% diol, no rutile could be detected at 600 °C, and at 700 °C, still only minor amounts of this phase are found. The fact, that the skeletal density of this sample is still below the theoretical density of anatase (Figure 5) suggests the existence of significant volume fractions of amorphous or at least strongly disordered TiO_2. In contrast to this, only rutile is found in powders from purely ethanolic solutions, even though these samples do not reach the theoretical skeletal density of rutile.

To explain this observation, we completed investigations by N_2 sorption experiments. Because the existence of macropores can be ruled out by SEM, open porosity can be estimated by combining the skeletal densities and the cumulative pore volumes. Generally, all systems are showing an evolution of surface area (Figure 7a) and open mesoporosity (Figure 7b) that has already been observed for sol−gel material.[21,22] The arising of microporosity and surface area at a calcination temperature of 350 °C is directly linked to the degradation of organics that leads to the skeletal densification (Figure 5). A further increase in the calcination temperature up to 400 °C leads to the formation of a mesoporous network that is densified at higher temperatures. However, with increasing 1,5-pentanediol content, especially with the addition of 20% 1,5-pentanediol, the surface area and porosity are significantly reduced above annealing temperatures between 400 and 500 °C. This faster densification process leads then to an incomplete thermal oxidative decomposition of organic residues, resulting in trapped elementary carbon.

In summary, a high densification rate caused by the addition of 1,5-pentanediol results in a dense microstructure with trapped elementary carbon. These impurities retard the phase transformation of anatase to rutile, as already reported for increasing concentration of other organic additives[23]like Pluronic. This effect may be utilized for the preparation of photocatalytic films, because only the anatase phase of TiO_2 is sufficiently active for such applications.[24]

3.2. Film Powders: General Consequences of a Large Surface-to-Volume Ratio and Air Moisture during Film Formation. According to the experimental approach outlined in Figure 1, the results obtained for sol powders have to be compared with experiments using material scraped from substrates after multiple coating experiments (film powders) in order to elucidate the changes induced by the large surface-to-volume ratio and the presence of air moisture during the dip-coating procedure. In the first step, film powder from a purely ethanolic solution will be investigated. In Figure 8, the thermogravimetric analysis and the differential thermal analysis of such a sample are given and compared with measurements carried out with the respective sol powders.

Up to temperatures between 350 and 400 °C, film powders and sol powders show similar mass losses under a constant heating rate of 10 K/min; the associated broad DTA signals both indicate exothermal decomposition reactions. Because these reactions are attributed to the oxidative decomposition of acetylacetonate groups, these organic residues were obviously stable against hydrolysis during film deposition under ambient conditions. Above 400 °C, the mass of film powders is diminished by only a few percent, and just a small exothermal peak is found in the DTA analysis. The ethanolate

(21) Löbmann, P.; Gross, J.; Glaubitt, W.; Fricke, J. *J. Non-Cryst. Solids* **1996**, *201*, 66.
(22) Krüger, R.; Glaubitt, W.; Löbmann, P. *J. Am. Ceram. Soc.* **2002**, *85*, 2827.
(23) Choi, H.; Dionysiou, D. *Prepr. Ext. Abstr. ACS Natl. Meet., Am. Chem. Soc., Div. Environ. Chem.* **2004**, *44*, 197.
(24) Fujishima, A.; Hashimoto, K.; Watanabe, T. *TiO_2 Photocatalysis: Fundamentals and Applications*; BKC Inc.: Tokyo, 1999.

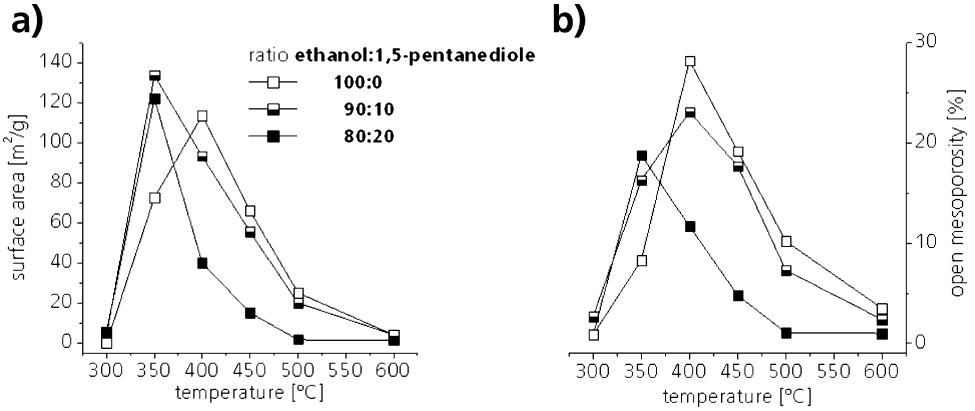

Figure 7. (a) Surface area and (b) open mesoporosity as a function of annealing temperature from sol powder prepared from sols containing 0, 10, and 20% 1.5-pentanediol, respectively.

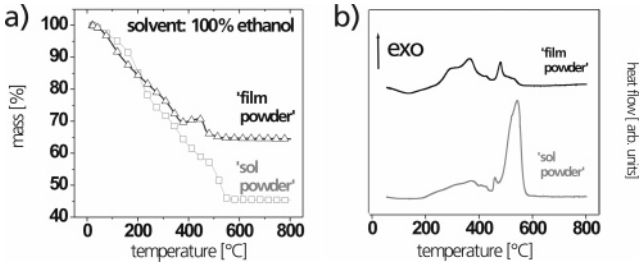

Figure 8. (a) Thermogravimetric analysis and (b) differential themal analysis of film powder obtained from a purely ethanolic coating solution (black lines). Additionally, the data of the respective sol powder from Figure 3 are given (gray lines). All experiments were performed undre a dry air atmosphere with a heating rate of 10 K/min.

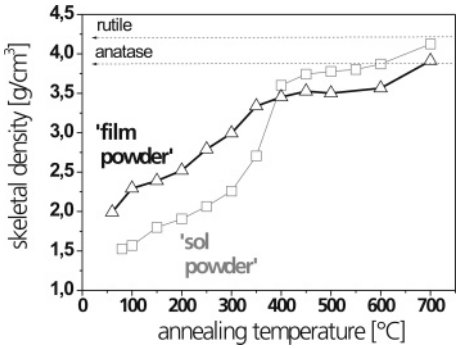

Figure 9. Skeletal density of film powder prepared from a purely ethanolic sol as a function of annealing temperature (△). For comparison, the data of the respective sol powder from Figure 4 are shown (□); the theoretical densities of rutile (4.24 g/cm^3) and anatase (3.83 g/cm^3) are given as references.

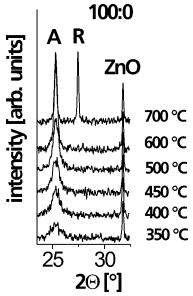

Figure 10. X-ray diffraction pattern of film powders prepared from purely ethanolic sols. The samples were annealed at temperatures between 350 and 700 °C, as indicated. ZnO was used as an external standard to normalize the signal intensities; peaks assigned to anatase (A) and rutile (R) are marked individually.

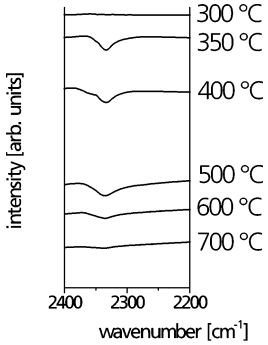

Figure 11. IR spectra of film powders that had been isothermally annealed for 1 h at the temperatures indicated.

groups, which are known to decompose in this temperature region, apparently underwent a hydrolytic cleavage during the coating procedure.

As a consequence of the lower content of residual organics, the film powder exhibits a higher skeletal density than the sol powder at low isothermal treatment temperatures (Figure 9). After annealing the samples at 400 °C, we measured densities around 3.5 g/cm^3 for the inorganic backbone of both samples regardless of their initial properties. Nevertheless, the sol powder goes through a better skeletal densification at higher temperatures.

This hindered densification of film powders correlates with the phase evolution of the material. Compared to the sol powders (Figure 6, left), a delayed formation of rutile (Figure 10) is observed.

Nevertheless, additional factors must be considered, because the densification of the film powder (Figure 9) proceeds at a lower level, as generally observed for the sol powders with comparable anatase:rutile ratios. IR spectra measured from the film powders (Figure 11) surprisingly indicate the presence of gaseous CO_2 in samples sintered between 350 and 600 °C. Because such results were never obtained for any precursor or sol powders, artifacts from faulty baseline corrections (atmospheric CO_2 in the beamline of the spectrometer) were ruled out.

To explain this observation, one has to consider that because of the high surface-to-volume ratio of the drying films, the densification of the material is much faster than the densification of sol powders prepared by rotational evaporation. Therefore, it is much more likely that some organics are trapped in the rapidly shrinking film. Upon annealing, some CO_2 as product of the thermal decomposi-

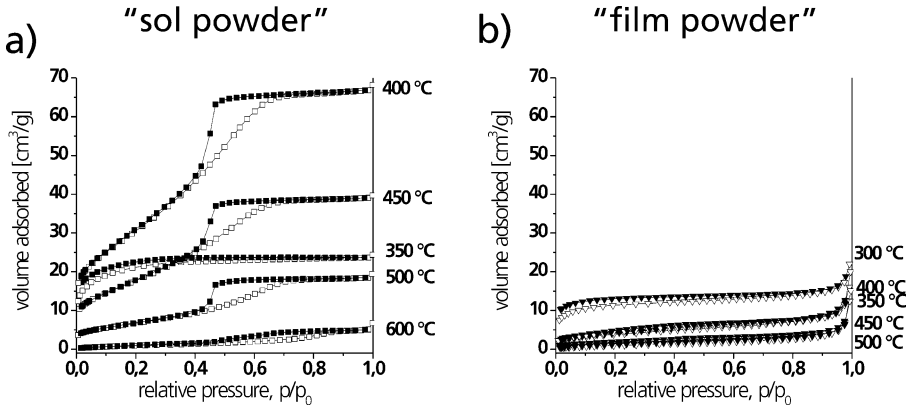

Figure 12. N2 adsorption isotherms for (a) sol powders and (b) film powders obtained from purely ethanolic solutions that had been isothermally annealed for 1 h at the temperatures indicated.

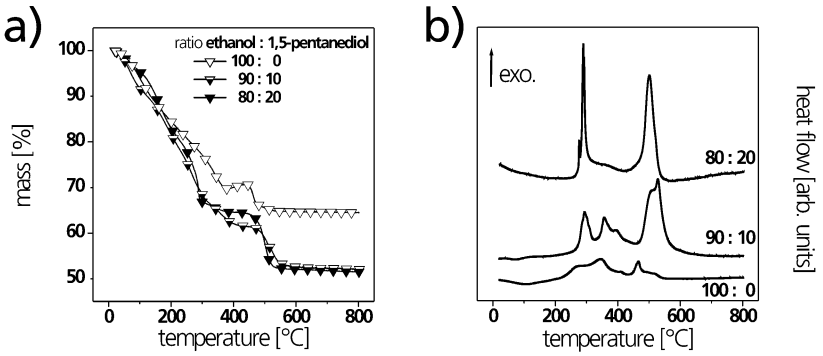

Figure 13. (a) Thermogravimetric analysis and (b) differential thermal analysis of film powder prepared from coating solutions that contained 0, 10, and 20% 1,4-pentanediol. All experiments were performed under a dry air atmosphere with a heating rate of 10 K/min.

tion[25] above 300 °C may be trapped in closed porosity within the film and is gradually removed during sintering above 500 °C. To support this assumption we require more microstructural information of the different materials.

Because sufficient amounts of film powders can be isolated by scraping material off dip-coated glass substrates, it is possible to perform N_2 adsorption experiments on isothermally sintered samples and compare the results with similarly treated sol powders (Figure 12). Indeed, sintered film powders exhibit a much denser microstructure than the respective sol powders, regardless of the annealing temperature. Only pores with diameters between 1 and 4 nm that give rise to Type I isotherms (Figure 12b) are generated by thermal treatment. Because closed pores, which contain gaseous CO_2, cannot be accessed by N_2 molecules, they are not expected to be detected.

Sol powders annealed at 350 °C also result in Type I isotherms. At 400 °C, these pores have been transformed to larger mesopores (type IV isotherms, diameters >3 nm according to BJH evaluation, data not shown). Similar formations of pore systems that are due to the removal of organic residues have been reported for xerogels[21] and sol−gel-derived fibers.[22] Between 450 and 500 °C, the volume of these pores is significantly reduced, and above 500 °C, the sol powders lose the porosity that is accessible to N_2 sorption experiments.

In conclusion, drying as a thin film results in the formation of closed pores and a much denser microstructure than in the respective sol powder. The resulting contamination with entrapped organic residues leads to a delayed phase transformation of anatase to rutile.

3.3. Changes Induced by the Solvent: Comparison between Different Film Powders. It is now important to investigate how these features of the film powders and thus the dip-coated films on glass are changed by the presence of 1,5-pentanediol. In Figure 13, thermogravimetric analyses and differential thermal analyses of different film powders are summarized. Samples prepared from coating solutions that contained 1,5-pentanediol undergo a stronger mass loss than the film powder isolated from the purely ethanolic system, but the overall oxide yield is about 50% for both samples regardless of the diol concentration in the initial sol.

As already shown in Figure 8b, the differential thermal analysis of film powders obtained from the coating solution based on pure ethanol presents the exothermal decomposition pattern typical for acetylacetonate groups between 200 and 400 °C followed by a weak signal that was assigned to residual ethanolate moieties (Figure 13). When the sols contain 1,5-pentanediol, this component is expected to be enriched during solvent evaporation (Figure 4) and film drying. The first DTA decomposition pattern (Figure 13b) between 200 and 400 °C is significantly altered when the sols contained 10% 1,5-pentanediol and consists of one sharp exothermal signal at 290 °C for higher content levels of the diol (80:20). When the respective sol powder was measured (Figure 4), this peak was partially superimposed by the endothermal evaporation of the diol. Thus, it can be concluded that the 1,5-pentanediol detected in Figure 13 is

(25) Colomban, P.; Bruneton, E. *J. Non-Cryst. Solids* **1992**, *147*−148, 201.

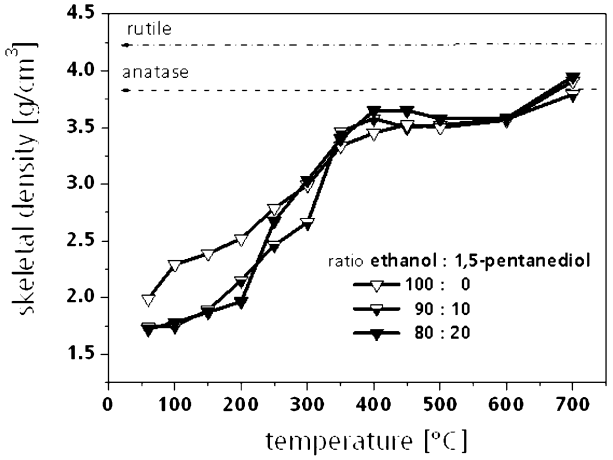

Figure 14. Skeletal densities of film powders prepared from sols containing 0 (▽), 10 (half-filled triangles), and 20% (▼) 1,5-pentanediol as a function of annealing temperature. The theoretical densities of rutile (4.24 g/cm^3) and anatase (3.83 g/cm^3) are given as references.

covalently linked to the film material. If the diol (bp 242 °C) is in equilibrium with acetylacetonate groups (bp AcAcH = 139 °C) during film drying, it is reasonable to assume that the more volatile component will preferably evaporate.

These chemical modifications also have an influence on the decomposition pattern at higher temperatures (Figure 13b). In contrast to material from purely ethanolic sols, the film powders prepared in the presence of the diol exhibit distinct exothermal signals above 500 °C that are assigned to alkoxy groups for sol powders (Figure 4). However, on the basis of Figure 13 only, it cannot be decided whether these peaks originate from 1,5-pentanediolate groups in a different chemical environment than those that decomposed around 300 °C or if the diol has a protective function for OEt moieties during drying of the film.

As already shown in Figure 9, film powders generally exhibit higher initial skeletal densities (Figure 14) after drying than the respective sol powders (Figure 5). Nevertheless, up to 250 °C, film powders prepared from sols containing 1,5-pentanediol show significantly lower skeletal densities than the respective material from purely ethanol-based sols (Figure 14), which can be directly attributed to the presence of the diol. Additionally, closed pores that contain gaseous CO_2 from the decomposition of organic residues decrease the backbone density of the film powders (see section 3.2).

Above 350 °C, all film powders started the formation of anatase (data not shown), but their further densification is significantly reduced compared to sol powders (Figure 9). Nevertheless, all film-powders show a microstructure that is not accessible to N_2 sorption experiments. The assumable internal stresses along with the presence of residual carbon delay the formation of rutile (data not shown), as already demonstrated for the sol powders.

The results obtained for the solid precursor material and the different sol and film powders can now provide the basis for a better understanding of the densification and formation of defects in the respective films prepared by sol−gel processing.

3.4. Thin films on Glass Deposited from Different Sols. Using different coating solutions, we prepared TiO_2 thin films on glass substrates by dip-coating. To compare samples that had undergone a comparable total densification, we determined coating conditions (withdrawal rates) in the foregoing experiments that led to films with similar film thickness after annealing at 600 °C. In Figure 15, the shrinkage of films from different coating solutions is given as a function of annealing temperature. As one would expect, the as-dried film from sols that contained only ethanol as solvent shows the smallest thickness, corresponding to the highest skeletal density of the respective film powder (Figure 14). Both coatings comprising 1,5-pentanediol show similar densification, as the data in Figure 14 would suggest.

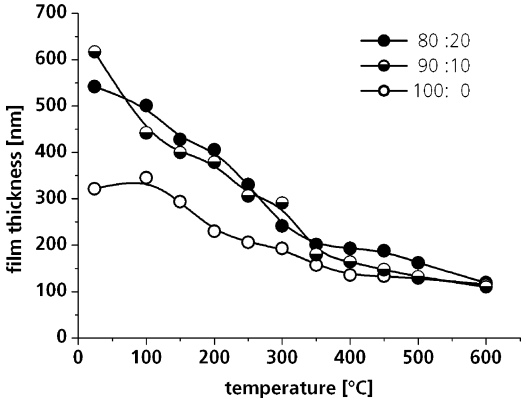

Figure 15. Thickness of TiO2 films on glass prepared from coating solutions containing 0 (○), 10 (◒), and 20% (●) 1,5-pentanediol as a function of annealing temperature. The films were prepared using withdrawal rates of 25, 18, and 11 cm/min, respectively, to achieve a film thickness of ∼110 nm for all series after annealing at 600 °C.

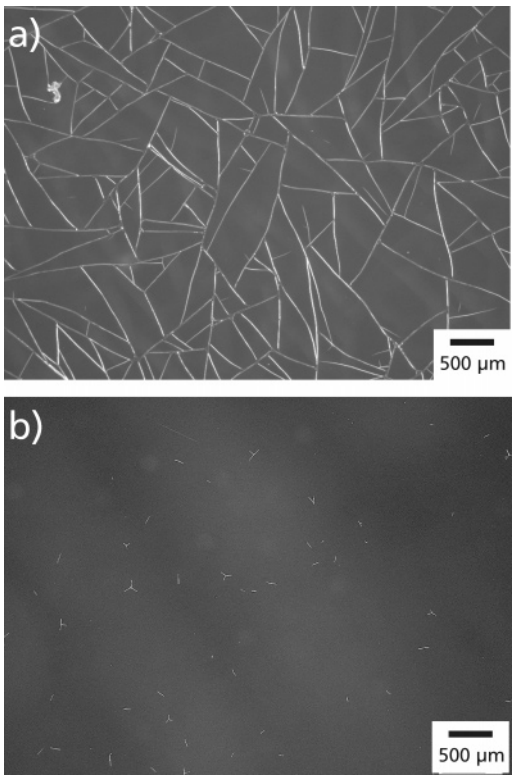

Figure 16. Light microscope surface images of TiO2 films on glass prepared from coating solutions containing (a) 0 and (b) 10% 1,5-pentanediol. Both samples were annealed at 600 °C for 10 min and have a final film thickness of ∼110 nm.

Nevertheless, the films show a quite different defect pattern, even though their thicknesses are basically identical (Figure 16). Film surfaces prepared from purely ethanolic

sols show a coarse crack pattern that separates undamaged film regions, with diameters often exceeding 500 μm (Figure 16a). These defects were presumably formed during the solvent evaporation and aging of the sol−gel film and can be observed within 2 min of drying time after the dip-coating.

The addition of 10 or 20% 1,5-pentanediol improves the film quality strongly, because only a few short cracks and starlike defects can be found. It has to be mentioned that Figure 16b was even taken from a relatively poor region near the edge of a 10×10 cm^2 substrate in order to facilitate focusing of the image at the single defects; most parts of the coated glass are virtually faultless. Because high-boiling diol is present, the films obviously maintain some plasticity during drying.

4. Conclusions

The use of soluble precursors and the preparation of powders scraped off the substrates after drying allowed for characterization of chemical and microstructural changes that take place during the densification of TiO_2 thin films.

When sols contain 1,5-pentanediol, this alcohol is partially incorporated in the precursor material during solvent evaporation both by rotational evaporation or during the drying of thin films. The materials thus have lower initial skeletal densities but undergo a more rapid solidification in an intermediate temperature region. As a result of fast densification, residual carbon is trapped and internal stresses are presumably induced.

The observations indicate that a rapid densification step, induced by either the chemical constitution of sol powders (presence of 1,5-pentanediol) or the fast solidification typical for film formation, generally delays the formation of rutile.

These results are a valuable tool for improved explanations for defects observed during drying and sintering of sol−gel films and an effective optimization of process parameters. Further studies are directed toward the quantitative analysis of defects, specific influence of heating rates, and formation of internal stresses as a function of solvent composition and air moisture.

Acknowledgment. The authors thank Helka Juvonen and Rémi Lemennais for performing numerous experiments. The generous support of Prinz Optics (Stromberg) by providing tailor-cut glass substrates is gratefully acknowledged.

CM052048N